High-Relaxivity Gadolinium-Modified High-Density Lipoproteins as Magnetic Resonance Imaging Contrast Agents

Karen C. Briley-Saebo,[†] Simonetta Geninatti-Crich,[‡] David P. Cormode,[†] Alessandra Barazza,[†,§] Willem J. M. Mulder,[†] Wei Chen,[†] Giovanni B. Giovenzana,[||] Edward A. Fisher,[§] Silvio Aime,[‡] and Zahi A. Fayad*[,†]

Molecular and Translational Imaging Institute, Mount Sinai School of Medicine, One Gustave Levy Place, P.O. Box 1234, New York, New York, University of Torino, Torino, Italy, New York University School of Medicine, New York, New York, and Universita del Piemonte Orientale, Novara, Italy

Received: December 9, 2008; Revised Manuscript Received: March 16, 2009

There is an ongoing desire to produce high-relaxivity, Gd-based magnetic resonance imaging (MRI) contrast agents. These may allow for lower doses to be used, which is especially important in view of the current safety concerns surrounding Gd in patients. Here we report the synthesis of a high-relaxivity MRI contrast agent, by incorporating Gd-chelating lipids that coordinate two water molecules into high-density lipoprotein ($q = 2$ HDL). We compared the properties of $q = 2$ HDL with those of an analogous HDL particle labeled with Gd-chelating lipids that coordinate only one water molecule ($q = 1$ HDL). We found that the $q = 2$ HDL possessed an elevated r_1 of 41 mM^{-1} s^{-1} compared to 9 mM^{-1} s^{-1} for $q = 1$ HDL at 20 MHz, but the $q = 2$ HDL exhibited high R_2* values at high fields, precluding imaging above 128 MHz. While carrying out this investigation we observed that enlarged, disrupted particles were formed when the synthesis was carried out above the lipid critical micelle concentration (cmc), indicating the importance of synthesis below the cmc when modifying lipoproteins in this manner. The high relaxivity of $q = 2$ HDL means it will be an efficacious contrast agent for future MR imaging studies.

Introduction

The development of contrast agents for medical imaging is a topic that attracts much attention. Magnetic resonance imaging (MRI) is a useful technique since it allows high-resolution images of patients to be acquired noninvasively and without exposure to ionizing radiation. However, the sensitivity of MRI toward contrast agents is relatively low, compared to other imaging techniques. As a result, many nanoparticle-based contrast agents are reported for MRI,[1−4] as nanoparticles can deliver large payloads of contrast-generating material. Such nanoparticles allow biological processes to be investigated in vivo, which is termed "molecular imaging".[5] A wide variety of Fe-[1] or Gd-labeled[2] nanoparticles have been reported as contrast agents for MRI. To the aim of performing molecular imaging in cardiovascular disease,[6] we have applied lipid-based nanoparticles such as micelles[7,8] or high-density lipoprotein (HDL).[9−12] In these prior HDL formulations we used dimyristoyl phosphatidylethanolamine modified with a diethylenetriamine pentaacetic acid Gd chelate (termed Gd−DTPA−DMPE, see Figure 1 for its structure) to provide image contrast.

The relaxivity of a contrast agent is a measure of its efficacy for MR image contrast production. There has always been a desire to increase the longitudinal relaxivity (r_1) of Gd-based contrast agents since the r_1 values of currently available commercial agents fall far short of what is theoretically possible.[13] By increasing r_1 values, the contrast generated increases thereby allowing for lower Gd doses to be used, decreasing the possibility of toxicity—the importance of this aspect is heightened due to the current safety concerns relating to chelated Gd contrast agents.[14] By increasing the efficacy of Gd chelates it may be possible to lower the dose and reduce the potential toxicity associated with Gd probes exhibiting prolonged circulation times.[14] In order to increase r_1 values, many groups have synthesized contrast agents with reduced tumbling rates ($1/\tau_r$) by attaching Gd chelates to the surface of nanoparticles or macromolecules.[15,16] In addition to altering τ_r, increases in the number of water proton binding sites to Gd (q) will also cause significant increases in the observed r_1 values. Due to the toxicity issues associated with Gd, however, it is critical that chelators bind Gd with high thermodynamic stability constants, an aim that often requires the chelator to bind to eight of the nine available coordination sites of Gd, leaving only one site available to coordinate a water molecule (i.e., $q = 1$).[17] This is the case for the commercially licensed Gd chelate of

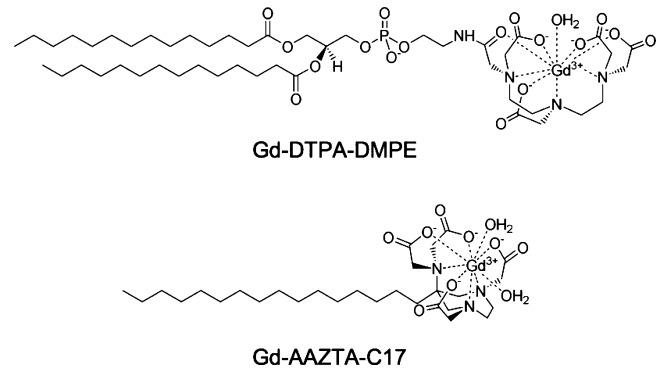

Figure 1. Chemical structures of the Gd-labeled lipids used in this study.

* Corresponding author. Tel.: 1 (212) 241-6858. E-mail: zahi.fayad@mssm.edu.
[†] Mount Sinai School of Medicine.
[‡] University of Torino.
[§] New York University School of Medicine.
[||] Universita del Piemonte Orientale.

10.1021/jp8108286 CCC: $40.75
Published on Web 04/10/2009

diethylenetriamine pentaacetic acid (DTPA), for example. Although tuning of both of τ_r and q have been pursued individually for increasing the r_1 value of a molecular imaging probe, it is relatively rare for both to be combined.[18,19]

Over the past 10−15 years, chelators that allow two to three water molecules to coordinate to Gd, yielding high relaxivities and forming stable complexes, have been reported.[20,21] One of the series of high-relaxivity Gd chelates that has been developed is based upon the heptadentate ligand 6-amino-6-methylperhydro-1,4-diazepinetetraacetic acid (AAZTA), which allows two water molecules to coordinate with the Gd metal ion, and is termed $q = 2$.[22,23] Despite the ability of this chelate to coordinate two water molecules, the Log K of the Gd(III) AAZTA complex is 20.2,[24] whereas that of the commercially available $q = 1$ Gd chelate Omniscan is 16.9,[25] which indicates Gd−AAZTA is sufficiently stable (where K is the formation constant of the gadolinium chelate in question). At 20 MHz, the r_1 value of [Gd−AAZTA]$^-$ was 7.1 s^{-1} mM^{-1} compared to 3.8 s^{-1} mM^{-1} observed for Gd−DTPA under similar experimental conditions.[22,23] The Gd−AAZTA complex has been modified with a 17 carbon atom alkyl chain (Gd−AAZTA−C17) that self-assembles into 5.5 nm micelles that exhibit a critical micelle concentration (cmc) of 0.1 mM and r_1 values of 30 s^{-1} mM^{-1} at 20 MHz.[23] Recently, it has been reported that Gd−AAZTA−C17 was incorporated into low-density lipoprotein (LDL), which was used as a vector for in vivo imaging of tumors.[19] For these reasons, it is hypothesized that incorporation of Gd−AAZTA−C17 into HDL will form stable, high-relaxivity nanoparticles that will potentially allow MR imaging of cardiovascular disease at lower doses.

The aim of the current study was to investigate the synthesis and characteristics of HDL labeled with Gd−DTPA−DMPE (a $q = 1$ amphiphile) or Gd−AAZTA−C17 ($q = 2$). The structures of these lipids are displayed in Figure 1. The labeled HDL was synthesized under ambient conditions and in the presence of β-cyclodextrin (β-CD) to establish the effect of the cmc on particle formation. The particles were characterized with dynamic light scattering, gel electrophoresis, relaxometric techniques, and a macrophage cholesterol of efflux ability. Relaxometric titration was performed in order to establish the association constants and binding capacity of the $q = 1$ and $q = 2$ complexes to native human HDL.

Experimental Section

Synthesis of Gd−DTPA−DMPE and Gd−AAZTA−C17 HDL. Gd−DTPA−DMPE ($q = 1$) (Avanti Polar Lipids, Inc. U.S.A.) and Gd−AAZTA−C17 ($q = 2$) (prepared according to established methods[23]) were incubated with native human HDL containing both the pre-β and spherical forms (Calbiochem, San Diego CA). Samples were prepared by first dissolving 2.4 μmol of the $q = 1$ or $q = 2$ complex in 30 mL of phosphate-buffered saline (PBS). The complex solution was warmed to 37 °C and added to 0.048 μmol (50:1) of warm human HDL and stirred for 2 h at 37 °C. The $q = 1$ and $q = 2$ labeled HDL was concentrated to a final volume of 1 mL using 10 000 molecular weight cutoff (MWCO) tubes, and the unincorporated gadolinium lipids were eliminated by washing three times with 5 mL of PBS in the same tubes. The final Gd concentration was determined by inductively coupled plasma mass spectrometry (ICP-MS) (Element-2, Thermo-Finnigan, Rodano (MI) Italy), and the protein concentration was determined by a commercial Bradford assay (Biorad). The incubation method used in the current study deviates from the methods described previously in the literature (incubation time reduced from 24 to 2 h).[9] The reduction in incubation time was based upon the kinetics and thermodynamics of the spontaneous exchange of amphiphiles between organized lipid aggregates. Studies indicate that the insertion rate constant of NBD-labeled DMPE into HDL (35 °C) was 8×10^4 M^{-1} s^{-1}.[26] As a result, the insertion of 2.4 μmol of $q = 1$ Gd−DTPA−DMPE into native HDL was presumed to occur within the 2 h incubation time frame used.

Relaxation Properties. Longitudinal and transverse relaxivities (r_1 and r_2) were determined at 20 MHz and 25 °C or 40 MHz and 37 °C using a Stelar Spinmaster (Mede, Pavia, Italy) and a Bruker Minispec (Bruker Medical GmbH, Ettingen, Germany), respectively. The relaxation rates (R_1 and R_2) were determined using standard inversion recovery and Carr−Purcell−Meiboom−Gill (CPMG) spin echo (echo time = 1 ms) sequences. Relaxivity values (r_1 and r_2) were obtained by measuring the R_1 and R_2 values at six different concentration levels of the $q = 1$ and $q = 2$ labeled HDL complexes in aqueous solution and by using the equation $R_{n(obs)} = R_{n(PBS)} + r_n[CA]$, where $R_{n(obs)}$ is the R_n in the presence of the contrast agent, $R_{n(PBS)}$ is the R_n of PBS without contrast agent, and [CA] is the contrast agent concentration. The error associated with the R_1 measurement (using both the Spinmaster and Bruker Minispec) was less than ±0.5%, and the slope of a linear correlation between the relaxation rates and Gd concentration defined the relaxivity values.

Proton R_1 and R_2 nuclear magnetic resonance dispersion (NMRD) profiles were measured over an applied magnetic field strength ranging from 0.00024 to 0.47 T (corresponds to a proton frequency of 0.01−20 MHz) using a Stelar field-cycling relaxometer operating at 25 °C. The error associated with the R_1 and R_2 measurement, using the Stelar Spinmaster, was ±1%.[23] Data points obtained over a frequency range of 20−70 MHz were collected using a Stelar Spinmaster spectrometer operated at variable field. Inversion recovery sequences with at least eight inversion times were used to obtain all R_1 values. R_2 values were obtained using a CPMG spin echo sequence with an echo time of 1 ms.

The effective transverse relaxation rate, R_2*, was determined in whole human blood at 63 MHz (Siemens Sonata) or 128 MHz (Siemens Allegra) using a multiple echo GRE sequence. Imaging was performed using a TR constant at 20 ms, and echo times ($n = 8$) ranged from 2.47 to 17.26 ms. The $q = 1$ and $q = 2$ labeled HDL was diluted in human blood (43% HCT, heparin anticoagulant) at four concentration levels ranging from 0 to 1.5 mM Gd. Plastic vials were fixed to the bottom of a glass phantom, and the phantom was filled with 2% agarose gel. After the agar was set, the plastic tubes were filled with blood spiked with $q = 1$ and $q = 2$ labeled HDL.

R_2* values were obtained from the fit of signal intensity versus echo time, as previously described.[27] The quantitative R_2* analysis was performed using a dedicated image-processing package (Efilm, Merge, Milwaukee, WI). The average R_2* values were determined for each sample, and dose−response curves were generated showing R_2* as a function of Gd concentration. R_2* values for 400 MHz were simulated via a linear extrapolation from the experimentally determined data.[28]

Stability and Binding Capacity. The cmc of the $q = 1$ and $q = 2$ complexes were investigated by measuring the R_1 values as a function of Gd concentration at 20 MHz and 25 °C in aqueous solution. For self-assembling lipids, a sharp increase in the R_1 value is observed when the system passes from a monomeric state to a micellar particle.[23]

The incorporation of the $q = 1$ and $q = 2$ complexes into native human HDL was determined by relaxometric titration,

as described previously.[29] In the current study the $q = 1$ or $q = 2$ complexes were titrated (at a fixed concentration of 0.09 and 0.07 mM, respectively) with an increasing amount of HDL (from 0 to 8×10^{-6} M). After heating for 2 h at 37 °C, the R_1 values were determined at 20 MHz and 25 °C. The binding strength or thermodynamic association constant (Ka), the number of binding sites (n), and the relaxivity of the macromolecular adduct (r_1) were derived from the change in R_1 with concentration via the PRE method.[29]

β-CD is known to dissociate and/or prevent micelle formation by exploiting the affinity of the lipophilic chains for the β-CD hydrophobic cavity.[30] The micelle disaggregation was followed by measuring the longitudinal relaxation rate decrease of a Gd−DTPA−DMPE 0.09 mM solution as a function of the β-CD concentration (from 0 to 0.014 M). A fixed amount of β-CD/Gd−DTPA−DMPE solution (7 and 0.07 mM, respectively) was titrated with HDL in order to hinder micelle formation and promote incorporation of the lipids into HDL (thereby pushing eq 1 to the right).

$$\beta\text{-CD/Gd-complex} + \text{HDL} \leftrightarrow \text{Gd-complex/HDL} + \beta\text{-CD} \quad (1)$$

Size. The hydrated mean diameter of the $q = 1$ and $q = 2$ HDL was determined using a Malvern dynamic light-scattering spectrophotometer (Malvern Instruments, Malvern, U.K.). All samples were analyzed at 25 °C in filtered (cutoff = 30 nm) HEPES buffer (pH = 7). The weighted z-average based on the number average was recorded.

The size range of the $q = 1$ and $q = 2$ adducts were also measured by nondenaturing gel electrophoresis using 4−20% polyacrylamide in 90 mM Tris, 80 mM boric acid, 3 mM azide, 3 mM EDTA buffer at 125 V for 24 h. Gels were prerun at 125 V prior to loading the samples. Both adducts were diluted (1:1) with a 20% sucrose and 0.25% bromophenol blue buffer solution prior to loading. All protein bands were visualized by commassie blue R-250 staining, and the particle size was determined by comparison with protein standards (high molecular weight calibration kit, Amersham Biosciences).

Macrophage Cholesterol Efflux. J774A.1 (ATCC, Manassas, VA) macrophages were incubated overnight with 15 μg/mL cholesterol and 0.5 μCi/mL [^{3}H]cholesterol in 0.2% bovine serum albumin−Dulbecco's modified Eagle's medium (BSA−DMEM). After an equilibration period of 3 h with 1 μg/mL of F-1394 in 0.2% BSA−DMEM, efflux was initiated by the addition of 50 μg/mL of HDL complexes by protein content. 100 μL aliquots of the medium were collected after 4 h, and the [^{3}H]cholesterol was measured by liquid scintillation counting (LSC). In order to measure the [^{3}H]cholesterol present in the cells, cell lipids were then extracted by incubating the cell monolayers overnight in isopropyl alcohol. After lipid extraction, the total [^{3}H]cholesterol present in lipid extract was measured by LSC and the efflux calculated as percentage of total.

Results

The R_1 and R_2 NMRD profiles obtained for the $q = 1$ and $q = 2$ labeled HDL formulations are shown Figure 2. The shape and amplitude of the R_1 NMRD profile for the $q = 1$ HDL adduct is similar to that observed for other Gd−lipid-based nanoparticles.[31−33] The R_1 and R_2 values obtained for the $q = 2$ HDL adduct were significantly greater than the values observed for the $q = 1$ adduct at all field strengths tested (for equivalent Gd concentrations). The relaxivity values obtained at 20 and 60 MHz are shown in Table 1, and maximum r_1 values were observed for both formulations at 20 MHz. At this field, the r_1 of $q = 2$ labeled HDL adduct was 3.5 times greater than that of $q = 1$ HDL formulation. The r_1 value obtained for $q = 2$ labeled HDL adduct was similar to the values obtained for Gd−AAZTA−C17 bound to fatted human serum albumin (HSA).[23] Whereas the size found for Gd−AAZTA−C17-labeled HDL was within the 7−13 nm size range of native HDL, the size found for Gd−DTPA−DMPE synthesized via this method was considerably larger (15.0 nm). The larger size of the $q = 1$ HDL was confirmed by gel electrophoresis (Figure 3).

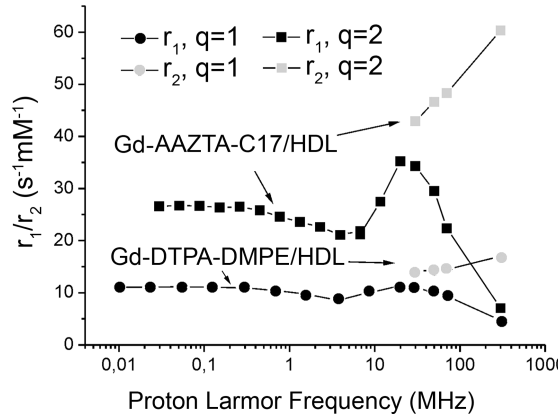

Figure 2. NMRD r_1 and r_2 profiles of the $q = 1$ Gd−DTPA−DMPE and $q = 2$ Gd−AAZTA−C17 HDL adducts in aqueous solution.

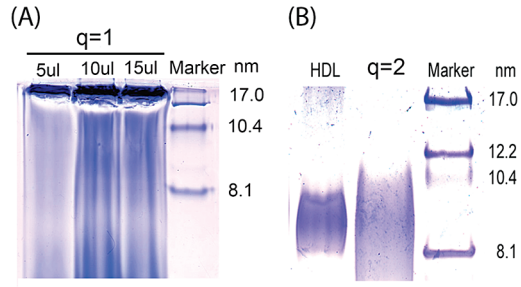

Figure 3. Nondenaturing gel electrophoresis of (A) $q = 1$ and (B) $q = 2$ HDL adducts relative to native HDL. The agents were applied at the top of the gels and ran down. The images were cropped to focus on the region of interest.

TABLE 1: Relaxation Properties and Size of Gd−DTPA−DMPE ($q = 1$) HDL and Gd−AAZTA−C17 ($q = 2$) HDL

		20 MHz			60 MHz		
HDL adduct	size (nm)	r_1 s^{-1} mM^{-1}	r_2 s^{-1} mM^{-1}	r_2/r_1	r_1 s^{-1} mM^{-1}	r_2 s^{-1} mM^{-1}	r_2/r_1
$q = 1$	15.0 ± 2.0	12	14	1.16	10.5	15	1.40
$q = 2$	10.8 ± 0.4	41	55	1.34	35.5	61	1.71

The r_2 values increased with increasing field strength (20−400 MHz) as shown in Figure 2 and Table 1. Due to the decrease in r_1 and increase in r_2, the r_2/r_1 ratios exhibited a dramatic increase at high magnetic fields (>60 MHz). The large r_2 values and high r_2/r_1 ratios indicate that significant T_2* effects (or susceptibility effects) may be present at high imaging field strengths. Therefore, the R_2* values of the $q = 1$ and $q = 2$ labeled HDL formulations were tested in phantoms at 63 and 128 MHz. As shown in Figure 4A, a nonlinear relationship between the Gd content and R_2* values was observed in human whole blood. The R_2* values generated for the $q = 2$ formulation were significantly greater than the values obtained for $q = 1$ labeled HDL adduct. In Figure 4B the effect of increasing field on the R_2* values for $q = 2$ HDL at different Gd concentrations is displayed, indicating the high R_2* values that will occur at

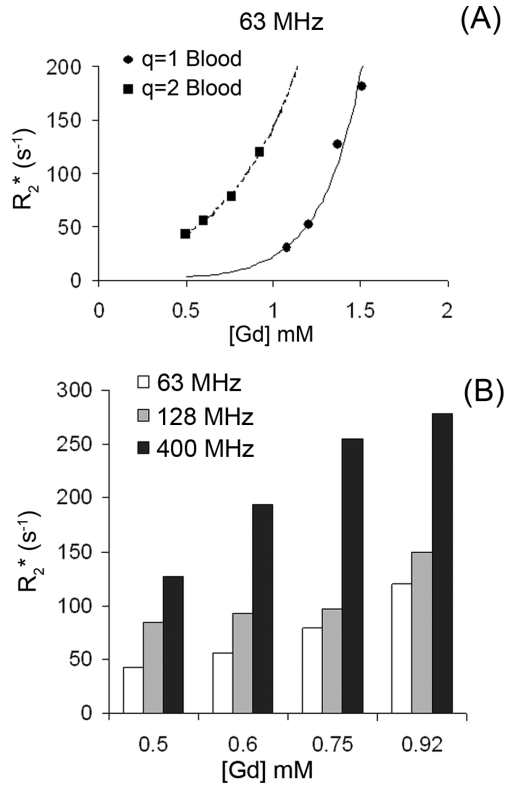

Figure 4. (A) R_2* of Gd−DTPA−DMPE (q = 1) HDL and Gd−AAZTA−C17 (q = 2) HDL in human blood at 63 MHz. (B) Comparison of R_2* values of differing concentrations of Gd−AAZTA−C17 HDL at 63, 128, and 400 MHz. The values for 400 MHz are derived from simulations.

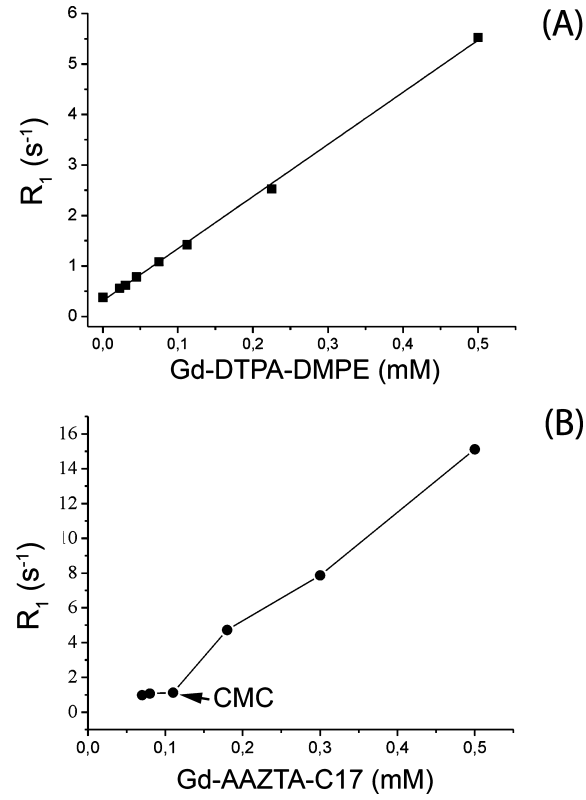

Figure 5. Effect of Gd−DTPA−DMPE (A) and Gd−AAZTA−C17 (B) lipid concentration on the longitudinal relaxation rate (R_1) in aqueous solution at 20 MHz. The critical micelle concentration (cmc) of Gd−DTPA−DMPE was lower than the detection limit of this method.

high field for q = 2 HDL, with R_2* values at 400 MHz around 100% greater than those found at 128 MHz (depending on the Gd concentration).

Figure 5 shows the effect of q = 1 and q = 2 lipid concentration on the R_1 values observed in aqueous solution. The cmc concentration of the q = 1 complex was lower than the minimal detectable concentration by relaxometric methods. The cmc value obtained for the q = 2 complex was similar to previously reported values (0.1 mM Gd).[23]

The titration of the q = 1 and q = 2 complexes with HDL (at pH = 7.4) is shown in Figure 6. Analysis of the relaxation data allowed for the determination of the binding strength (Ka), number of binding sites (n), and relaxivity of the adduct (r_1), as displayed in Table 2. The binding affinity of the q = 2 complex to HDL was significantly greater than the affinity observed by the q = 1 complex. The number of binding sites along with the Ka values indicate that (1) the q = 2 lipids integrate into the HDL particle and (2) the low cmc associated with the q = 1 Gd−DTPA−DMPE lipid may induce detergent perturbation thereby resulting in the formation of larger HDL (fused HDL) species, as depicted in Figure 7.[34] The formation of fused HDL could explain the larger size of the q = 1 Gd−DTPA−DMPE HDL adduct as measured by both light scattering (Table 1) and gel electrophoresis (Figure 3), although other models may explain these results. The mean diameter of the q = 1 HDL was significantly greater than both the q = 2 HDL adduct and native HDL.[35]

In order to investigate whether the q = 1 complex forms a fused HDL adduct, competitive titrations with β-CD were performed. As shown in Figure 8, β-CD is able to dissociate the q = 1 lipid micelles, as reflected in the decreasing R_1 values with increasing β-CD concentration (as the β-CD complex has

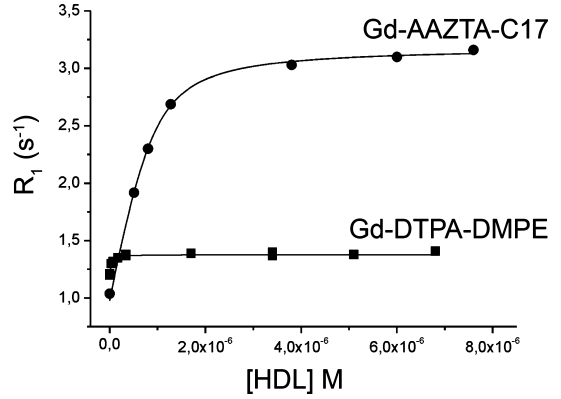

Figure 6. Titration of native human spherical HDL into Gd−DTPA−DMPE (q = 1, 0.09 mM) or Gd−AAZTA−C17 (q = 2, 0.07 mM). The samples were incubated for 2 h at 25 °C prior to R_1 measurement at 20 MHz.

a faster tumbling rate and hence a lower relaxivity than the micelle form of Gd−DTPA−DMPE). When HDL is titrated into a solution containing both the q = 1 complex and β-CD, the binding affinity increases and the number of binding sites decreases, which is indicative of lipid incorporation into the HDL nanoparticle, as shown in Table 2. For the q = 2 adduct (that exhibits a higher cmc value and is able to integrate into the lipoprotein), the presence of β-CD did not significantly affect the binding affinity and number of binding sites. However, if the q = 2 lipid is incubated with HDL at lipid concentrations greater than the cmc concentration, formation of a fused HDL particle (indicative of detergent perturbation) was observed, as demonstrated by the Ka and high n values (Table 2).

TABLE 2: Thermodynamic Association Constant (Ka), the Number of Binding Sites (n), and the Relaxivity of the Adduct (r_1) at 20 MHz Were Calculated from Titration of HDL into Solutions of Either Gd−DTPA−DMPE or Gd−AAZTA−C17[a]

	titration of HDL to Gd complex			titration of HDL in the presence of β-CD		
complex	Ka (M^{-1})	n	r_{1p} (s^{-1} mM^{-1})	Ka (M^{-1})	n	r_{1p} (s^{-1} mM^{-1})
$q = 1$	$1.7 \pm 1 \times 10^4$	2500 ± 500	11.2 ± 0.5	$>10^6$	65 ± 2	8.5 ± 0.3
$q = 2$	$7 \pm 1 \times 10^4$	80 ± 5	41 ± 0.5	$7.0 \pm 1.4 \times 10^4$	75 ± 6	41 ± 0.6
$q = 2$ >cmc	$1.2 \pm 0.8 \times 10^2$	1250 ± 750	37 ± 1			

[a] The titration was repeated in the presence of 7 mM β-CD. >cmc represents the synthesis of the $q = 2$ HDL adduct at lipid concentrations above the critical micellular concentration (cmc).

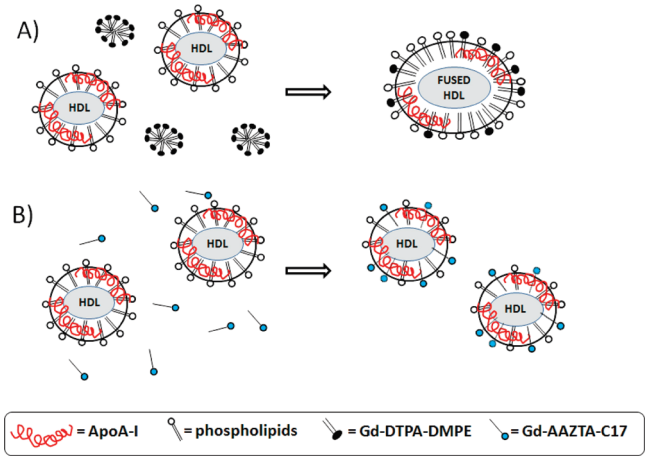

Figure 7. Schematic depiction of the formation of $q = 1$ Gd−DTPA−DMPE (A) and $q = 2$ Gd−AAZTA−C17 (B) HDL adducts. Gd−DTPA−DMPE forms a micelle prior to interaction with the native spherical HDL surface. Gd−AAZTA−C17, however, integrates into the lipid layer associated with HDL.

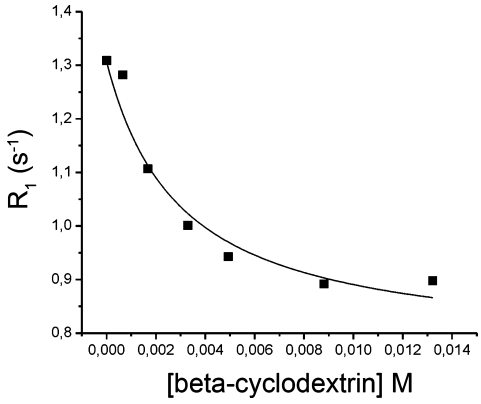

Figure 8. Effect of β-cyclodextrin (β-CD) concentration on the R_1 values obtained for 0.09 mM Gd−DTPA−DMPE in aqueous solution (20 MHz).

No significant difference was observed between the $q = 1$ and $q = 2$ HDL formulations with respect to cholesterol efflux from macrophages in vitro, as shown in Figure 9. The presence of the paramagnetic complex did, however, cause a ca. 25% reduction (relative to native HDL) in the ability of the lipoproteins to extract cholesterol from these cells. The reduced efficacy may be related to the electrostatic charge associated with Gd−DTPA−DMPE (−2) and Gd−AAZTA−C17 (−1) lipids. Integration or interaction of these charged lipids into or on the native lipoprotein may decrease the total net charge of the particle thereby hindering the ability to extract cholesterol from the cells. However, significant efflux potential was retained for these modified particles.

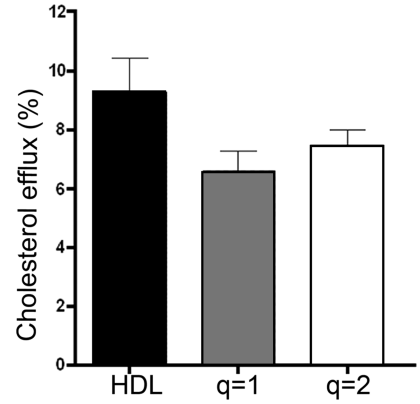

Figure 9. Cholesterol efflux associated with J774A.1 macrophages following incubation with native human HDL Gd−DTPA−DMPE ($q = 1$) HDL, and Gd−AAZTA−C17 ($q = 2$) HDL.

Discussion

The current study demonstrates the use of Gd−AAZTA−C17 as a high-relaxivity $q = 2$ Gd chelate for the MR labeling of native HDL. The integration of the $q = 2$ Gd−AAZTA−C17 lipid into native HDL resulted in the formation of a high-relaxivity molecular imaging probe with r_1 values 3.5 times greater than the $q = 1$ HDL adduct (Table 1, Figure 2) and 8−9 times greater than the commercially available octadentate contrast agents (i.e., Gd−DTPA, Gd−DTPA−BMA). It should be noted, however, that the Gd−DTPA−DMPE chelate is a monoamide and hence likely has a relatively slow water exchange rate,[36] which could limit relaxivity of the Gd−DTPA−DMPE HDL particle. The high r_2 values along with the R_2* results obtained in blood (Figure 4), strongly suggest that T_2* effects may modulate the MR signal observed for the $q = 2$ HDL adduct at high field strengths. The origin of the T_2* increase is the consequence of susceptibility effects typical for slowly moving particles loaded with a high number of paramagnetic ions. These effects scale up with the magnetic field strength. In order to optimize the full potential of the $q = 2$ labeled HDL formulation, it will be preferential to perform in vivo imaging studies at clinically relevant fields (<128 MHz) where r_1 values are high and r_2 and r_2* values are relatively low. The design of the Gd−AAZTA−C17 lipid used in this study could be improved by the addition of another acyl chain, as lipophilic gadolinium complexes bearing monoacyl chains have been linked to hemolytic effects.[37]

The results of the current study also show that successful integration of Gd lipids into native HDL was strongly dependent upon the cmc concentration of the amphiphile used. At lipid concentrations below the cmc (or when β-CD is present to hinder micelle formation) the lipids were easily integrated into the lipoproteins, and stable HDL adducts with high stability constants (Table 2) were formed. At Gd−DTPA−DMPE concentrations above the cmc, larger HDL species with a

relatively wide size distribution were formed (though only one species was observed). These particles had a higher relaxivity than particles synthesized below the cmc, which could be related to the larger size as larger particles tumble more slowly, leading to increased relaxivity. Micelles formed from Gd−DTPA−DMPE have a diameter of 6 nm, so this larger size measured is not due to an artifact of detecting Gd−DTPA−DMPE only micelles.

The reason for this larger-sized HDL formed at concentrations above the cmc is unclear, but it may be due to detergent perturbation induced formation of fused HDL species as suggested by Pownall.[34] In these studies, exposure of HDL to cholate above the cmc values resulted in the loss of ApoA-I and phospholipid from the lipoprotein surface. The loss of these structures exposes the neutral lipid core to the surrounding aqueous phase thereby inducing the fusion of two or more ApoA-I/phospholipid-depleted HDL particles, as depicted in Figure 7. The fusion of the HDL adducts (induced by incubation with the $q = 1$ lipid above the cmc) is supported by the larger size of the $q = 1$ HDL adducts obtained (Figure 3) and also by the higher number of binding sites (n) observed with Gd−DTPA−DMPE (Table 2). Detergent perturbation was not observed for the $q = 2$ lipid, when incubations with HDL were performed at concentrations below the $q = 2$ lipid cmc values. This finding is in agreement with the cholate studies that show HDL fusion only occurs at cholate concentrations above the cmc.[34] As shown in Table 2, if HDL is incubated with the $q = 2$ lipid above the cmc value, then HDL particles with the characteristics of fusion are observed.

The importance of the cmc on lipid insertion into the HDL particle is further demonstrated by the results observed when β-CD was present during synthesis of the $q = 1$ HDL adduct. The addition of β-CD to the Gd−DTPA−DMPE solution caused the disruption of micelle formation due to the interaction of β-CD with the aliphatic chains of the complex (Figure 8). The resultant monomeric Gd−DTPA−DMPE/β-CD adduct formed effectively raises the cmc.[34] After addition of HDL, equilibrium between the monomeric Gd−DTPA−DMPE/β-CD adducts and Gd−DTPA−DMPE/HDL particles was established. Since the stability of Gd−DTPA−DMPE/HDL particle was higher, the equilibrium shifted toward the formation of an integrated $q = 1$ HDL adduct (Table 2).

Cholesterol efflux measures the ability of the lipoprotein to bind and transport cholesterol out of macrophages. The efflux potential is not only important from a therapeutic point of view (reduction of cholesterol deposition in the arterial wall) but is also indicative of how the modification affects lipoprotein function. The addition of the charged paramagnetic label reduced (by approximately 25%) the cholesterol efflux capacity observed in J774A.1 macrophages, relative to native HDL (Figure 9). Therefore, lipid modification (either by $q = 1$ or $q = 2$ addition) influenced lipoprotein function. The reduction in cholesterol efflux may be due to a more negative particle charge relative to native HDL (both Gd−AAZTA−C17 and Gd−DTPA−DMPE are negatively charged lipids). Studies have indicated that increasing the negative charge of HDL may stimulate hydrolysis by reducing association with hepatic lipase.[38] As a result, future studies are planned to investigate the effect of charge on cholesterol efflux.

The incorporation of a high-relaxivity $q = 2$ lipid into modified HDL represents an advance in the potential clinical translation of this platform. Although prior studies clearly show that $q = 1$ HDL adducts are effective contrast agents for the detection of vulnerable atherosclerotic plaque, there are concerns related to toxicity for long-circulating Gd-labeled agents.[14] By increasing the MR efficacy of the Gd-based chelates by the use of high-relaxivity complexes (such as Gd−AAZTA−C17) we hypothesize that it may be possible to significantly reduce the dosage of Gd required and thereby limiting concerns related to Gd toxicity.

Conclusions

Incorporation of $q = 2$ Gd−AAZTA−C17 into the lipid layer of native HDL resulted in the formation of a high-relaxivity, stable, integrated HDL adducts. Due to the low cmc associated with the $q = 1$ Gd−DTPA−DMPE lipids, incubation with native HDL resulted in the formation of fused HDL adducts due to detergent perturbation. Future studies will investigate the diagnostic potential of the $q = 2$ HDL adduct at clinical field strengths (63 MHz).

Acknowledgment. Partial support was provided by NIH/NHLBI RO1 HL71021 and NIH/NHLBI HL78667 (Z.A.F.). S.A. acknowledges support from MIUR (FIRB RBIP06293N), EU_Meditrans project (NMP4-CT-2006-026668), and DiMi (DIMI-LSHB-CT-2005-512146).

Supporting Information Available: Titration curves for Gd−DTPA−DMPE and Gd−AAZTA−C17 into HDL into β-CD and for Gd−AAZTA−C17 above the cmc. This material is available free of charge via the Internet at http://pubs.acs.org.

References and Notes

(1) Corot, C.; Robert, P.; Idee, J.-M.; Port, M. *Adv. Drug Delivery Rev.* **2006**, *58*, 1471.
(2) Mulder, W. J. M.; Cormode, D. P.; Hak, S.; Lobatto, M. E.; Silvera, S.; Fayad, Z. A. *Nat. Clin. Pract. Cardiovasc. Med.* **2008**, *5*, S103.
(3) Lanza, G. M.; Winter, P. M.; Caruthers, S. D.; Hughes, M. S.; Cyrus, T.; Marsh, J. N.; Neubauer, A. M.; Partlow, K. C.; Wickline, S. A. *Nanomedicine* **2006**, *1*, 321.
(4) Bulte, J. W. M.; Kraitchman, D. L. *NMR Biomed.* **2004**, *17*, 484.
(5) Weissleder, R.; Mahmood, U. *Radiology* **2001**, *219*, 316.
(6) Briley-Saebo, K. C.; Mulder, W. J. M.; Mani, V.; Hyafil, F.; Amirbekian, V.; Aguinaldo, J. G. S.; Fisher, E. A.; Fayad, Z. A. *J. Magn. Reson. Imaging* **2007**, *26*, 460.
(7) Amirbekian, V.; Lipinski, M. J.; Briley-Saebo, K. C.; Amirbekian, S.; Aguinaldo, J. G.; Weinreb, D. B.; Vucic, E.; Frias, J. C.; Hyafil, F.; Mani, V.; Fisher, E. A.; Fayad, Z. A. *Proc. Natl. Acad. Sci. U.S.A.* **2007**, *104*, 961.
(8) Briley-Saebo, K. C.; Shaw, P. X.; Mulder, W. J.; Choi, S. H.; Vucic, E.; Aguinaldo, J. G.; Witztum, J. L.; Fuster, V.; Tsimikas, S.; Fayad, Z. A. *Circulation* **2008**, *117*, 3206.
(9) Frias, J. C.; Williams, K. J.; Fisher, E. A.; Fayad, Z. A. *J. Am. Chem. Soc.* **2004**, *126*, 16316.
(10) Frias, J. C.; Ma, Y.; Williams, K. J.; Fayad, Z. A.; Fisher, E. A. *Nano Lett.* **2006**, *6*, 2220.
(11) Cormode, D. P.; Briley-Saebo, K. C.; Mulder, W. J. M.; Aguinaldo, J. G. S.; Barazza, A.; Ma, Y.; Fisher, E. A.; Fayad, Z. A. *Small* **2008**, *4*, 1437.
(12) Cormode, D. P.; Skajaa, T.; van Schooneveld, M. M.; Koole, R.; Jarzyna, P.; Lobatto, M. E.; Calcagno, C.; Barazza, A.; Gordon, R. E.; Zanzonico, P.; Fisher, E. A.; Fayad, Z. A.; Mulder, W. J. M. *Nano Lett.* **2008**, *8*, 3715.
(13) Raymond, K. N.; Pierre, V. C. *Bioconjugate Chem.* **2005**, *16*, 3.
(14) Sieber, M. A.; Pietsch, H.; Walter, J.; Haider, W.; Frenzel, T.; Weinmann, H. J. *Invest. Radiol.* **2008**, *43*, 65.
(15) Mulder, W. J. M.; Koole, R.; Brandwijk, R. J.; Storm, G.; Chin, P. T. K.; Strijkers, G. J.; Donega, C. D.; Nicolay, K.; Griffioen, A. W. *Nano Lett.* **2006**, *6*, 1.
(16) Zhang, Z.; Greenfield, M. T.; Spiller, M.; McMurry, T. J.; Lauffer, R. B.; Caravan, P. *Angew. Chem., Int. Ed.* **2005**, *44*, 6766.
(17) Caravan, P. *Chem. Soc. Rev.* **2006**, *35*, 512.
(18) Datta, A.; Hooker, J. M.; Botta, M.; Francis, M. B.; Aime, S.; Raymond, K. N. *J. Am. Chem. Soc.* **2008**, *130*, 2546.
(19) Crich, S. G.; Lanzardo, S.; Alberti, D.; Belfiore, S.; Ciampa, A.; Giovenzana, G.; Lovazzano, C.; Aime, S. *Neoplasia* **2007**, *9*, 1046.
(20) Bligh, S. W. A.; Drew, M. G. B.; Martin, N.; Maubert, B.; Nelson, J. *J. Chem. Soc., Dalton Trans.* **1998**, 3711.

(21) Pierre, V. C.; Botta, M.; Aime, S.; Raymond, K. N. *Inorg. Chem.* **2006**, *45*, 8355.

(22) Aime, S.; Calabi, L.; Cavallotti, C.; Gianolio, E.; Giovenzana, G. B.; Losi, P.; Maiocchi, A.; Palmisano, G.; Sisti, M. *Inorg. Chem.* **2004**, *43*, 7588.

(23) Gianolio, E.; Giovenzana, G. B.; Longo, D.; Longo, I.; Menegotto, I.; Aime, S. *Chem.—Eur. J.* **2007**, *13*, 5785.

(24) Baranyai, Z.; Uggeri, F.; Giovenzana, G. B.; Bényei, A.; Brüker, E.; Aime, S. *Chem.—Eur. J.* **2009**, *15*, 1696.

(25) Cacheris, W. P.; Quay, S. C.; Rocklage, S. M. *Magn. Reson. Imaging* **1990**, *8*, 467.

(26) Estronca, L. M. B. B.; Moreno, M. J.; Laranjinha, J. A. N.; Almeida, L. M.; Vaz, W. L. C. *Biophys. J.* **2005**, *88*, 557.

(27) Mani, V.; Briley-Saebo, K. C.; Itskovich, V. V.; Samber, D. D.; Fayad, Z. A. *Magn. Reson. Med.* **2006**, *55*, 126.

(28) Haacke, E. M.; Brown, R. W.; Thompson, M. R.; Venkatesan, R. *Magnetic Resonance Imaging Physical Principles and Sequence Design*; John Wiley & Sons, New York, NY, 1999.

(29) Aime, S.; Chiaussa, M.; Digilio, G.; Gianolio, E.; Terreno, E. *J. Biol. Inorg. Chem.* **1999**, *4*, 766.

(30) Joseph, J.; Dreiss, C. A.; Cosgrove, T.; Pedersen, J. S. *Langmuir* **2007**, *23*, 460.

(31) Kimpe, K.; Parac-Vogt, T. N.; Laurent, S.; Pierart, C.; Vander Elst, L.; Muller, R. N.; Binnemans, K. *Eur. J. Inorg. Chem.* **2003**, 3021.

(32) Parac-Vogt, T. N.; Kimpe, K.; Laurent, S.; Pierart, C.; Elst, L. V.; Muller, R. N.; Binnemans, K. *Eur. J. Inorg. Chem.* **2004**, 3538.

(33) Hovland, R.; Glogard, C.; Aasen, A. J.; Klaveness, J. *Org. Biomol. Chem.* **2003**, *1*, 644.

(34) Pownall, H. J. *Biochemistry* **2005**, *44*, 9714.

(35) Nichols, A. V.; Krauss, R. M.; Musliner, T. A. *Methods Enzymol.* **1986**, *128*, 417.

(36) Toth, E.; Burai, L.; Brucher, E.; Merbach, A. E. *J. Chem. Soc., Dalton Trans.* **1997**, 1587.

(37) Anelli, P. L.; Lattuada, L.; Lorusso, V.; Schneider, M.; Tournier, H.; Uggeri, F. *MAGMA (NY)* **2001**, *12*, 114.

(38) Boucher, J. G.; Nguyen, T.; Sparks, D. L. *Biochem. Cell Biol.* **2007**, *85*, 696.

JP8108286